Available online at www.sciencedirect.com
SCIENCE DIRECT®
Polymer 45 (2004) 3701–3708
polymer
www.elsevier.com/locate/polymer

Regeneration of *Bombyx mori* silk by electrospinning. Part 2. Process optimization and empirical modeling using response surface methodology

Sachiko Sukigara[a], Milind Gandhi[b], Jonathan Ayutsede[c], Michael Micklus[c], Frank Ko[c,*]

[a]*Faculty of Education and Human Sciences, Niigata University, 8050 Igarashi 2 no cho, Niigata city, Niigata 950-2181, Japan*
[b]*School of Biomedical Engineering, Sciences and Health System, Drexel University, Philadelphia, PA 19104, USA*
[c]*Fibrous Materials Research Laboratory, Department of Materials Science and Engineering, Drexel University, 31st and Market street, Philadelphia, PA 19104, USA*

Received 17 September 2003; received in revised form 17 March 2004; accepted 18 March 2004

Abstract

The response surface methodology was used to model and optimize the electrospinning parameters for the spinning of regenerated nanoscale silk fibers from domestic silkworm, *Bombyx mori*. Electric field and silk concentrations were chosen as variables to control fiber diameter at different spinning distances. Fiber diameter was correlated to these variables by using a second order polynomial function. The predicted fiber diameters were in agreement with the experimental results. Response surfaces were constructed to identify the processing window suitable for producing nanoscale fibers.

Keywords: Electrospinning; Silk; Response surface methodology

1. Introduction

Protein based biopolymers, such as silk are of great interest to the biotechnologists as well as the material scientists due to their unique combination of structural and biocompatible properties. The anti-parallel β pleated structure of silk gives rise to its structural properties of combined strength and toughness [1]. Its biocompatibility makes it an ideal candidate for biomedical applications [2]. Silk has been used as suture material for many years. The natural silk fibers spun by *Bombyx mori* are 10–20 μm in diameter and consist of a pair of triangular core proteins covered by a coating protein (sericin) that glues silk fibers together. While the triangular cross-section of silk is of great attribute for making highly reflective textile clothing, it may not be desirable for suture material because of possible damage to the tissues. Since the natural living systems are made up of fibrils at nanoscale levels and organized in a hierarchical manner, it is of interest to examine the morphology, chemical and mechanical properties of silk not only at much smaller diameter (nanoscale) but also in different geometrical shape (cylindrical) for biomaterial application.

Electrospinning is a unique method capable of producing nanoscale fibers from both synthetic [3–6] as well as natural polymers for biomedical applications. Nanoscale polymeric fibrous materials are the fundamental building blocks of living systems. The scientific understanding of the materials at nanoscale level allows us to control the basic properties of materials without changing their chemical composition. Utilization of this technology presents the opportunity to develop new families of products for biomedical and biotechnology applications. Nanofibers have unique properties, which include high surface area to volume ratio, strength, surface energy, as well as thermal and electrical conductivity. Polymer nanofibers have potential applications as membrane filters, scaffolds for tissue regeneration, wound dressings and drug delivery [7]. The nanoscale regenerated silk fibers can be tailor-made to create new geometric and functional properties, which are unavailable in the natural silk fiber. Motivated by the potential benefits

* Corresponding author. Tel.: +1-2158951640; fax: +1-2158956684.
E-mail address: fko@coe.drexel.edu (F. Ko).

0032-3861/$ - see front matter © 2004 Elsevier Ltd. All rights reserved.
doi:10.1016/j.polymer.2004.03.059

gained by the regeneration of silk in the nanoscale, several attempts were made to electrospin silk from various sources such as silkworm cocoon silk, spider (*Nephila Clavipes*) dragline silk and recombinant hybrid silk-like polymer with fibronectin functionality [8–12]. In spite of the growing interest, to date no systematic study has been reported on the optimum processing parameters required to generate nanoscale fiber reproducibly and continuously by electrospinning.

In part one of our study we identified the important electrospinning processing parameters that affect fiber morphology and diameter of regenerated silk nonwoven mat [10]. Silk proteins are biosynthesized in the epithelial cells of the specialized glands of *Lepidoptera*. These proteins are then secreted into the lumen of these glands, where the proteins are stored prior to spinning into fibers. The liquid crystalline silk polymer is then concentrated in the silk ducts by removal of salt and water [13]. In an attempt to mimic this procedure, we prepared the spinning dope of regenerated silk by filtration, dialysis and lyophilization of commercial silk fibers.

We have empirically determined that the silk solution concentration was the dominant parameter in producing uniform and continuous fibers. Uniform fibers (less than 100 nm diameter) were obtained from 12 to 15% (w/w) silk in formic acid concentrations and electric fields of 3 and 4 kV/cm [10]. In order to obtain a more systematic understanding of these process conditions and to establish a quantitative basis for the relationships between electrospinning parameters and fiber diameter, response surface methodology (RSM) [14] was employed in this study.

RSM has been used successfully for material and process optimization [14] in numerous studies including thermoplastic elastomers [15], diamond-like carbon films [16] and poly(vinyl alcohol) hydrogels [17]. This approach has the advantage of taking into account the combined effects of several parameters and it uses statistical methods to fit an empirical model to the experimental data. The use of a model to describe the effects of electrospinning parameters allows us to represent the influencing parameter in a simple and systematic way and to predict the results of the experiments with different parameter combinations. Thus, RSM enables us to obtain an overview of the processing parameters and their influence on each other. Furthermore, it helps us to obtain the surface contours of these parameters using experimental and predicted values. These contour plots outline the processing window and point out the direction to attain the optimum condition in the form of an Eigen value. For more detailed explanation on RSM see Refs. [14,18]. A brief introduction is provided herein.

1.1. Response surface methodology

RSM is used in situations where several variables influence a feature (called the response) of the system. The steps in the procedure are described briefly as follows.

1. Identification of variables $\zeta_1, \zeta_2, \zeta_3 \ldots$ for response η.
2. Calculation of corresponding coded variables $(x_1, x_2, x_3 \ldots)$ by using the following equation.

$$x_i = \frac{\zeta_i - [\zeta_{Ai} + \zeta_{Bi}]/2}{[\zeta_{Ai} - \zeta_{Bi}]/2} \quad (1)$$

   where ζ_{Ai} and ζ_{Bi} refer to the high and low levels of the variables ζ_i, respectively.
3. Determination of the empirical model by multiple regression analysis to generate theoretical responses $(\hat{y})$. The second-order model is widely used in RSM. The general equation for response η of the second-order model is given by:

$$\eta = \beta_0 + \sum_{i=1}^{k} \beta_i x_i + \sum_{i=1}^{k} \beta_{ii} x_i^2 + \sum \sum_{i<j=2}^{k} \beta_{ij} x_i x_j \quad (2)$$

   where k is the number of factors, x_i are the coded variables and β are coefficients.
4. Calculation of the coefficients β to fit the experimental data as close as possible.

The relationship between the response and the variables is visualized by a response surface or contour plot to see the relative influence of the parameters, to find an optimum parameter combination, and to predict experimental results for other parameter combinations.

The electric fields and concentrations are the two variables identified in our study. When $k = 2$, the empirical model from the general Eq. (2) becomes

$$y = \beta_0 + \beta_1 x_1 + \beta_2 x_2 + \beta_{11} x_1^2 + \beta_{22} x_2^2 + \beta_{12} x_1 x_2 + \varepsilon \quad (3)$$

where

y is the natural logarithm of the fiber diameter,
x_1 is the coded electric field variable,
x_2 is the coded concentration variable, and
ε is the random error term.

RSM procedure to optimize the process parameters for the electrospinning silk is shown in Fig. 1.

The purpose of this paper is to identify the optimum combination of electric field and polymer concentration in order to produce silk fibers with diameters less than 100 nm. To investigate the interaction of these variables and tip-to-collection plate distance (referred in this paper as spinning distance), the experiments were regulated at two spinning distances. It is our objective to use this empirical model to guide our future experiments and to spin uniform nanoscale fibers for future applications.

2. Experimental

2.1. Materials and electrospinning

B. mori silk fibroin fibers (Pfaltz and Bauer Inc.) were

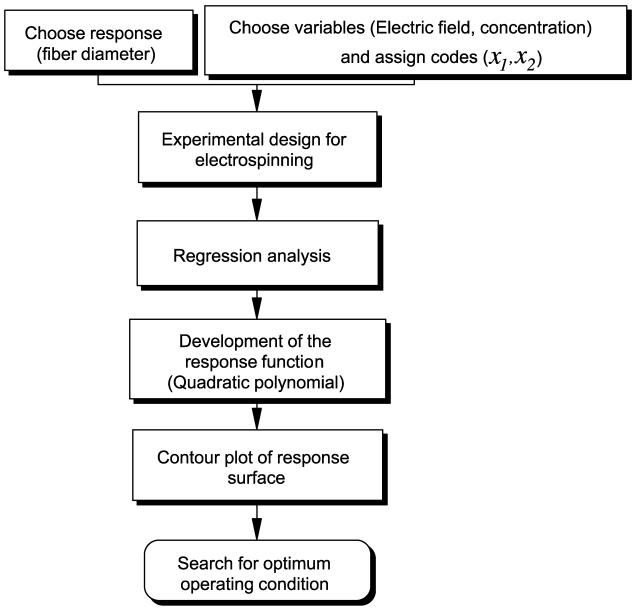

Fig. 1. RSM procedure to optimize the electrospinning condition of regenerated silk.

dissolved in 50% aqueous $CaCl_2$ and dialyzed against deionized water. All concentration measurements were done in weight by weight (w/w). All chemicals were obtained from Sigma-Aldrich. Following lyophilization the regenerated silk fibroin sponge, dissolved in formic acid (98–100%), was placed in a 3 ml syringe having 18-G needle. The silk–formic acid solution was electrospun at a 45° spinning angle, a voltage of 10–35 kV and a constant spinning distance of either 5 or 7 cm. The formic acid evaporated as the solution jet proceeded to the collection plate, leaving behind fibers or beads, depending on the silk concentration. Details of spinning dope preparation and electrospinning conditions were reported in our previous paper [10].

The fiber morphology was examined by field emission environmental scanning electron microscope (Phillips XL-30 ESEM). For each experiment, fiber diameter and distribution were determined from 100 measurements of the random fibers.

2.2. Experimental design

A factorial experiment was designed using two factors (electric field and concentration). For the application of RSM to develop the process, sequential experiments were carried out. Initially, we designed the experiment at the spinning distance of 7 cm then other spinning distances were considered. Our previous study showed that the effect of spinning distance on fiber diameter between 7 and 10 cm (15% silk concentration) was insignificant. Thus, a lower spinning distance of 5 cm was used for subsequent experiments. These experiments were planned according to the modified central composite design [14]. This type of design defines the minimum number of experimental combinations in the experimental domain to be explored in order to obtain the maximum information for adjusting the proposed model. For a quadratic model, experiments must be performed for at least three levels of each factor. These levels are best chosen equally spaced. The two factors (silk concentration and electric field) and three levels resulted in nine possible combinations of factor settings. A schematic of the experimental design is shown in Fig. 2(A) and (B). The values in the bracket are coded variables (x_1 : electric field, x_2 : concentration) and the numbered values at coordinate point represents the mean fiber diameter obtained by experiment. The coded values were calculated using Eq. (1) of the electric field (ζ_1) and concentration (ζ_2). In this case, the high value of the electric field (ζ_{A1}) is 4 kV/cm and the low value is 2 kV/cm (ζ_{B1}). The high value of the concentration is 20% (ζ_{A2}) and the low value is 10% (ζ_{B2}). In the case of 5 cm spinning distance, the critical concentration for fiber formation was above 12% and there were no fibers formed at concentrations of 10% or less. This resulted in an uneven spacing of the levels as can be seen in Fig. 2(B). Coded and natural variables are listed in Table 1.

Table 1
Design of experiments (variables and levels)

Experiment	Coded variables		Natural variables	
	x_1	x_2	Electric field, ζ_1 (kV/cm)	Concentration, ζ_2 (%)
Spinning distance: 5 cm				
1	−1	−0.6	2	12
2	−1	0	2	15
3	−1	1	2	20
4	0	−0.6	3	12
5	0	0	3	15
6	0	1	3	20
7	1	−0.6	4	12
8	1	0	4	15
9	1	1	4	20
Spinning distance: 7 cm				
1	−1	−1	2	10
2	−1	0	2	15
3	−1	1	2	20
4	0	−1	3	10
5	0	0	3	15
6	0	1	3	20
7	1	−1	4	10
8	1	0	4	15
9	1	1	4	20

3. Results

3.1. Response function

By linear regression analysis of Eq. (3) the numerical values for coefficients ($\beta_0, \beta_1, \beta_2, \beta_{11}, \beta_{22}, \beta_{12}$) were

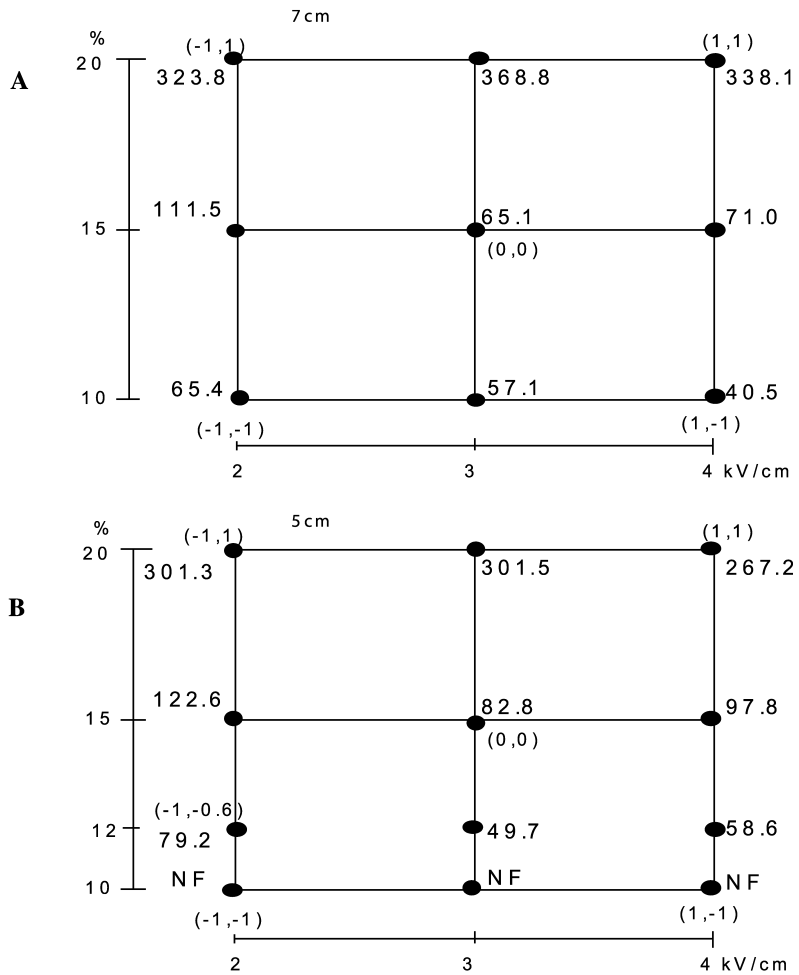

Fig. 2. Experimental design (A) spinning distance 7 cm and (B) spinning distance 5 cm. The values at the coordinate points show the mean fiber diameter (nm) of 100 measurements and coded values are shown in the brackets (electric field and concentration). NF: no fiber formation.

obtained. The fitted second-order equation for the natural logarithmic fiber diameter is given by

$$\hat{y} = 4.484 - 0.115x_1 + 0.907x_2 + 0.178x_1^2 + 0.159x_2^2 + 0.05616x_1x_2 \quad (4)$$

for 5 cm spinning distance and

$$\hat{y} = 4.362 - 0.148x_1 + 0.931x_2 + 0.03334x_1^2 + 0.523x_2^2 + 0.131x_1x_2 \quad (5)$$

for 7 cm spinning distance.

P-values (a measure of the statistical significance) and R^2 (a measure of the percent of the response being represented by the variables) for regression models (Eqs. (4) and (5)) are shown in Table 2. *P*-values for both regressions are less than the significance level of 0.05, validating adequacy of these models. Values of R^2 are 0.947 for 5 cm spinning distance and 0.958 for 7 cm spinning distance. The models predict a variability of 95% in new data for 5 cm spinning distance and 96% for 7 cm spinning distance.

3.2. Response surfaces of fiber diameter as a function of concentration and electric field

3.2.1. Effects of concentration on fiber diameter

Fig. 3 shows contour plots in the case of 7 cm spinning distance. The response indicates that changes in fiber diameter are more responsive to electric field at the low solution concentration. Low concentration of fibroin gives low fiber diameters. Concentration of 10% gives fiber diameters ranging from 35 to 80 nm while a 20% concentration of fibroin gives fiber diameters above

Table 2
Significance probability (*P*-value) and correlation coefficient of linear regression for response surface equations

Spinning distance (cm)	*P*-value	*R*	Adjusted R^2
5	0.006	0.984	0.947
7	0.007	0.992	0.958

$y = \beta_0 + \beta_1x_1 + \beta_2x_2 + \beta_{11}x_1^2 + \beta_{22}x_2^2 + \beta_{12}x_1x_2 + \varepsilon$.

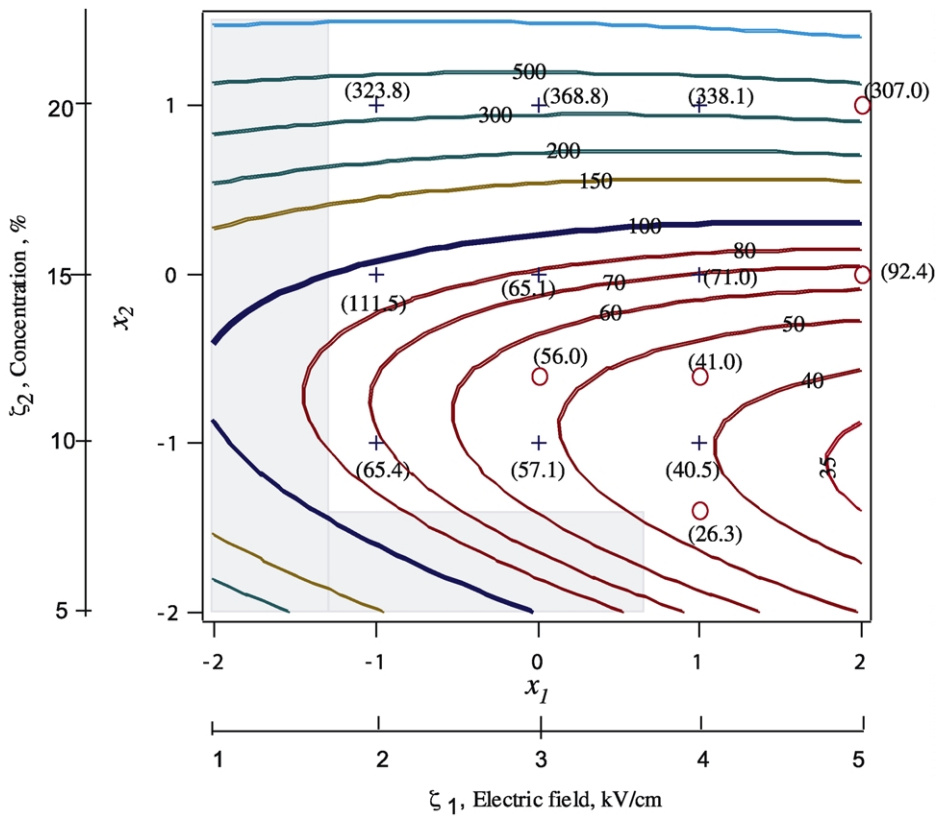

Fig. 3. Contour plots of fiber diameters (nm) as a function of electric field and solution concentration for 7 cm spinning distance. The corresponding experimental mean fiber diameters (nm) are placed in the contour plot (symbol + at experimental design and symbol ○ at new experiments). Fibers are not formed in the shaded area.

300 nm. The interaction effect of the electric field can also be observed. The corresponding experimental mean fiber diameters used to build this function are shown in Fig. 3 (symbol +). The residual (difference between the experimental fiber diameters and the predicted fiber diameter) is less than the standard deviation of the predicted fiber diameters. In Fig. 3, five points (symbol ○) show the corresponding experimental mean fiber diameters from new experiments. The residuals at these conditions are also less than the standard deviation of the experimental fiber diameters except one combination (4 kV/cm, 8%). However, this result follows the direction obtained from contour plots suggesting that the lower concentration gives lower fiber diameter. The responses, however, are iso-level curve response (Fig. 3), indicating that nanofibers can be produced over a range of process conditions. Fig. 3 also shows that nanofibers can be theoretically produced at low concentrations (less than 8%) and at low electric fields (less than 2 kV/cm) but this was not possible experimentally indicating that one should not extrapolate from empirical models.

3.2.2. The effects of electric field on fiber diameter

The contour plot for the 7 cm spinning distance shows that the fiber diameter decreases as the electric field is increased at a given or fixed silk concentration. For a 10% concentration, increasing the electric field from 1 to 5 kV/cm leads to a decrease in the fiber diameter from 100 to 35 nm. Keeping the electric field constant, an increase in the concentration increases the fiber diameter in the spinnable region. At a higher concentration, the effect of the electric field becomes negligible. This is apparent from the slopes of the curves, which become smaller as the concentration increases. For example, at 20% the fiber diameter is ~500 nm irrespective of the electric field. Thus, electric field has more effect on the fiber diameter at low concentrations of silk.

3.2.3. The optimum processing window for nanofibers

The center of the response surface system called the stationary point is a point representing minimum values of the response or the smallest fiber diameter. The stationary point is mathematically described [14] by the following Eqs. (6) and (7).

The fitted regression model, Eq. (4), in matrix notation

$$\hat{y} = b_0 + \mathbf{x}'\mathbf{b} + \mathbf{x}'\hat{\mathbf{B}}\mathbf{x} \tag{6}$$

where b_0, $\mathbf{b}$, $\hat{\mathbf{B}}$ are estimates of the intercept, the linear, and the second-order coefficients, respectively. $\mathbf{x}' = [x_1, x_2]$ and $\hat{\mathbf{B}} = 2 \times 2$ symmetric matrix.

The stationary point $\mathbf{x}_s$ is obtained by

$$\mathbf{x}_s = -\hat{\mathbf{B}}^{-1}\mathbf{b}/2 \tag{7}$$

The stationary points were calculated using Eq. (7). For spinning distance of 7 cm the coded values are $\mathbf{x}_s = [5.263, -1.549]$ and $\hat{y} = 3.25$. The corresponding physical values are 8.3 kV/cm (electric field), 7.3% (concentration) and 25.8 nm (fiber diameter). Although this condition is outside of the experimental design region, it indicates the direction chosen for process conditions to obtain the smaller fiber diameter. In the case of 7 cm spinning distance, lower concentration with higher electric field produces smaller fiber diameter.

3.2.4. Effect of spinning distance on fiber diameter

The experiments for 5 cm spinning distance was designed to confirm the region producing nanofibers found in the case of the 7 cm spinning distance. As shown earlier (Fig. 2), a 7 cm spinning distance exhibits larger fiber producing region than a 5 cm spinning distance from experiments.

Fig. 4 shows the contour plots of fiber diameter calculated in the case of 5 cm spinning distance. High concentrations of fibroin lead to large fiber diameter that is consistent with the trend observed in the case of 7 cm spinning distance. Concentration of 20% forms fibers with diameters in the 300–500 nm range. A lower concentration of 12% produces fibers with diameters in the 150–60 nm range. At a given or fixed concentration of fibroin, the combined effect of the electric field is seen to cause reduction in fiber diameter, as was observed in the case of the 7 cm spinning distance. For a 12% concentration, an increase in electric field from 1 to 5 kV/cm results in reduction in fiber diameter from 150 to 60 nm. The values of mean fiber diameter from 100 measurements are also shown at corresponding conditions (symbol +, Fig. 4). The residual is less than the standard deviation of the experimentally obtained fiber diameters.

Comparing fiber diameters at 5 and 7 cm spinning distances at the same electric field and concentration (see Figs. 3 and 4) shows that fiber diameters obtained at 7 cm spinning distance are lower than those at 5 cm spinning distance in the concentration range of 10–18%. For 12% silk concentration, an increase in electric field from 2 to 4 kV/cm leads to a decrease in fiber diameter from 70 to 45 nm and from 76 to 56 nm for 7 and 5 cm spinning distances, respectively. The difference is greater at higher electric field (5 kV/cm). One might suggest that this result is due to the longer spinning distance which enables the polymer to evaporate solvent more efficiently even at the same electric field strength thus leading to smaller fiber diameter in comparison with the diameter obtained at 5 cm spinning distance. However, higher concentration such as 20% and at an electric field of less than 4 kV/cm, the fiber diameters obtained for 7 cm spinning distance were larger than those for a 5 cm spinning distance. This result might suggest that a critical point has been reached at this concentration whereby interaction effects of smaller

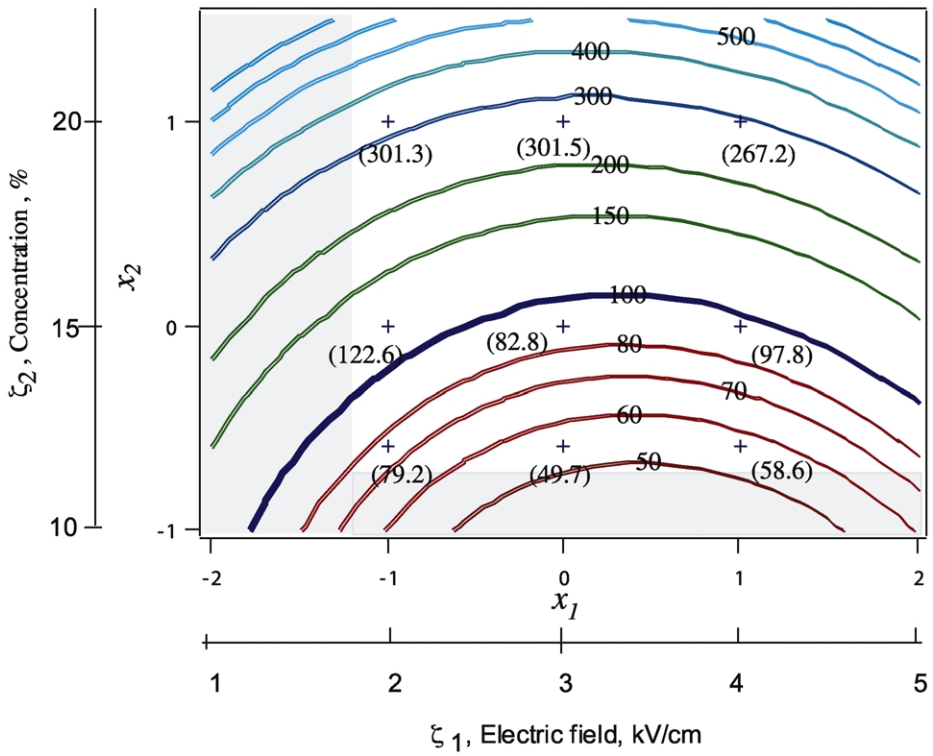

Fig. 4. Contour plots of fiber diameters (nm) as a function of electric field and solution concentration for 5 cm spinning distance. Corresponding experimental values of mean fiber diameters (nm) are placed in the contour plot with symbol +. Fibers are not formed in the shaded area.

spinning distance and electric field lead to a decrease in fiber diameter size.

4. Discussion

The use of RSM to study the optimum combinations of electrospinning parameters to produce nanofibers from regenerated silk was introduced. Contour plots relating fiber diameter to electric field and solution concentration were generated for spinning distances of 5 and 7 cm. These plots will assist in future studies and production of electrospun nanoscale silk fibers.

The response surfaces indicated that silk nanofibers (less than 100 nm) could be produced from solutions in the range of 10–16.5% concentration with electric fields above 2 kV/cm and for 7 cm spinning distance. For a spinning distance of 7 cm the contour plot predicted the fiber diameter of less than 40 nm. In our experiment, fibers (diameter less than 30 nm) were electrospun at 10%, 3 kV/cm and 7 cm spinning distance as shown in Fig. 5. However, experimental results indicated that the electrospun nonwoven mat contain beads at a concentration of 10% or less (see Fig. 6(A)). In order to produce fibers without beads concentrations above 12% are required as seen in Fig. 6(B).

From the fact that different contour shapes were obtained for 5 and 7 cm spinning distances, these results might suggest a coupling effect or interaction between spinning distance and electric field strength, which should also be considered when a simple normalization to electric field (voltage/spinning distance) is used.

The use of the stationary point to determine the optimum combinations of the electric field and concentration to generate nanofibers gives a usual indication of a trend, but must be used with caution as often some values fall beyond the experimental region. The stationary point for a spinning distance of 5 cm is $\mathbf{x}_s = [0.79, -2.9]$, physical values were 3.8 kV/cm and 0.04%. This stationary point at 5 cm spinning distance represents the condition under which fibers cannot be formed because silk concentration is too low. In such a case, further experiments with broader range may be designed to improve the process.

It must be noted that variations may exist in the properties of *B. mori* silk obtained from different sources or processed differently. These differences for the natural polymer may cause variations in experimental results.

5. Conclusions

RSM analysis was applied to the experimental results to develop a processing window which will produce nanoscale regenerated silk fibers by electrospinning process. Contour plots relating fiber diameter to electric field and solution concentration were generated for spinning distances of 5 and 7 cm. From the RSM models, a concentration of 8–10% and electric field of 4–5 kV/cm were found to be the sufficient condition for achieving nanofibers of diameters less than 40 nm. The difference between the experimental

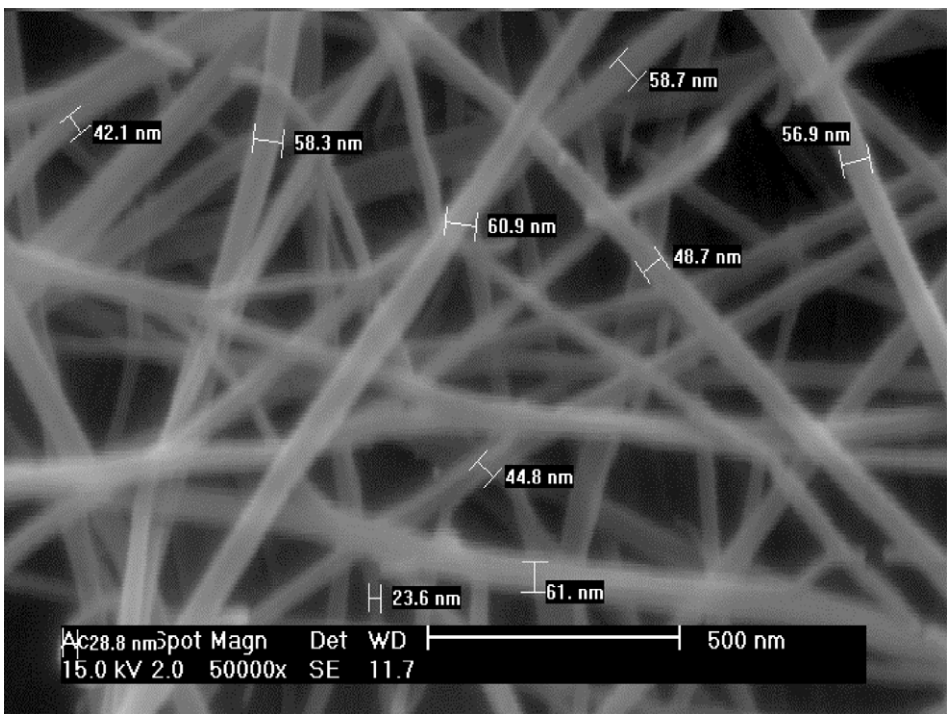

Fig. 5. The morphology of fibers at a spinning concentration of 10%, an electric field of 3 kV/cm and a spinning distance of 7 cm.

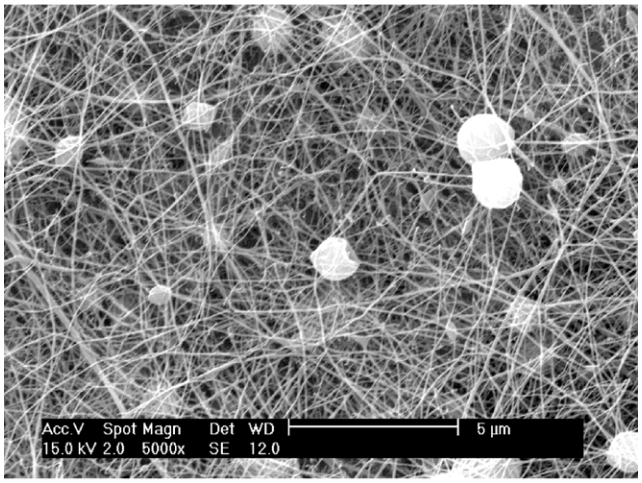

Fig. 6. The morphology of fibers at two different conditions. (A) Concentration 10%, electric field 4 kV/cm and spinning distance 7 cm and (B) concentration 15%, electric field 5 kV/cm and spinning distance 7 cm.

fiber diameters and the predicted fiber diameters is less than the standard deviation of the experimental fiber diameters. The model will serve as a useful guide to obtain uniform nanoscale silk fibers in future at various combinations of process variables and to construct the response surfaces for mechanical, chemical and physical properties.

The characterization of the properties of an electrospun nonwoven silk mat will be reported in a subsequent paper.

Acknowledgements

This work was made possible by a visiting scholarship provided to Sachiko Sukigara by the Ministry of Education, Culture, Sports, Science and Technology through Niigata University in Japan. This project is supported in part by the State of Pennsylvania under the Nanotechnology Institute.

References

[1] Altman GH, Diaz F, Jakuba C, Calabro T, Horan RL, Chen J, Lu H, Richmond J, Kaplan DL. Biomaterials 2003;24:401–16.
[2] Panilaitis B, Altman GH, Chen J, Jin HJ, Karageorgiou V, Kaplan DL. Biomaterials 2003;24:3079–85.
[3] Doshi J, Reneker D. J Electrostat 1995;35:151–60.
[4] Jin HJ, Fridrikh SV, Rutledge GC, Kaplan DL. Biomacromolecules 2002;3:1233–9.
[5] Li WJ, Laurencin CT, Caterson EJ, Tuan RS, Ko F. J Biomed Mater Res 2002;4:613–21.
[6] Zong X, Kim K, Fang D, Ran S, Hsiao BS, Chu B. Polymer 2002;43:4403–12.
[7] Huang ZM, Zhang YZ, Kotaki M, Ramakrishna S. Compos Sci Technol 2003;63:2223–53.
[8] Ohgo K, Zhao C, Kobayashi M, Asakura T. Polymer 2003;44:841–6.
[9] Kim SH, Nam YS, Lee TS, Park WH. Polym J 2003;35(2):185–90.
[10] Sukigara S, Gandhi M, Ayutsede J, Micklus M, Ko F. Polymer 2003;44:5721–7.
[11] Zarkoob S, Reneker DH, Eby RK, Hudson SD, Ertley D, Adams WW. Polym Prepr 1998;39(2):244–5.
[12] Buchko CJ, Chen LC, Shen Y, Marthin DC. Polymer 1999;40:7397–407.
[13] Vollrath F, Knight DP. Nature 2001;29:541–8.
[14] Myers RH, Montgomery DC. Response surface methodology: process and product optimization using designed experiments. New York: Wiley-Interscience; 1995.
[15] Lopez-Manchado MA, Arroyo M. Polymer 2001;42:6557–63.
[16] Wachter R, Cordery A. Carbon 1999;37:1529–37.
[17] Trieu H, Outubuddin S. Polymer 1995;36:2531–9.
[18] Davies OL. The design and analysis of industrial experiments. NY: Hafner Publishing Company; 1956.